

## Impedance Behavior of Some Reactive Systems in Aprotic Solvents

Hossnia S. Mohran

Chemistry Department, Faculty of Science, 82524 Sohag, Egypt

**Abstract:** AC-Impedance Spectroscopic (IS) measurements in the frequency range  $10 \text{ Hz} \leq f \leq 50 \text{ kHz}$  for some reactive systems such as diphenylanthracene (DPA), ferrocene and anthraquinone are investigated. The experiments are carried out in pure and dry dichloromethane ( $\text{CH}_2\text{Cl}_2$ ), acetonitrile ( $\text{CH}_3\text{CN}$ ) and N,N- dimethylformamide (DMF) containing tetrabutylammonium perchlorate (TBAP) as supporting electrolyte. The IS diagrams of these systems are characterized in the complex plane by either straight lines passing through the origin or a high frequency capacitive and in most cases, a low-frequency Warburg behavior. The IS parameters are calculated and discussed.

**Key words:** Charge transfer resistance, warburg coefficient, impedance behavior, reactive systems

### INTRODUCTION

Electrochemical impedance spectroscopy (EIS) has been very successfully applied to investigate a multitude of systems<sup>[1]</sup>. Epelboin *et al.*<sup>[2]</sup> have published the original work on the system iron- $\text{H}_2\text{SO}_4$ -propargylic acid. The study has stimulated interest in the use of impedance technique for the determination of polarization resistances. The numerous unique advantages<sup>[3]</sup> of the technique have been overshadowed through its difficulties in the interpretation of the data obtained<sup>[4]</sup>. Some researchers have even come to the limiting conclusion that the method is only valid for uniform corrosion problems<sup>[5]</sup>. It has been recognized for a long time that AC techniques are valuable in which diagnostic conclusions can be drawn to elucidate an electrode reaction mechanism, although not many practical applications in this field have been reported.

The theory was firstly discussed by Gerischer<sup>[6]</sup>, in the form of faradaic impedance at equilibrium potential. Studies at non-equilibrium potentials were made by Aylward *et al.*<sup>[7]</sup>. Smith and coworkers<sup>[8,9]</sup> have given more general theories in terms of the amplitude of the faradaic admittance and its phase angle as a function of d.c. potential.

Comprehensive studies, treating many different mechanistic electrode reaction routes, have been solved and reported<sup>[9,10]</sup>. Theories with experimental examples for the electrode impedance in the case that the electroactive species are specifically adsorbed at the electrode-solution interface were also discussed<sup>[11,12]</sup>. On the coupling of interfacial and diffusional impedances, De Levie *et al.* treated the diffusion problem without explicit boundary conditions<sup>[13, 14]</sup>.

Since a complete survey of the studies applying the AC measurements to electrode reaction kinetics is not possible, a few basic examples are listed<sup>[15-17]</sup>.

Beer *et al.* studied the electrochemical properties of mono- and di-ferrocenyl bipyridyl ligands containing trans conjugated olefinic linkages between the ferrocene redox centres and the 4,4'-substituted 2,2'-bipyridine moieties<sup>[18]</sup>. Sulcliffe *et al.* described the use of the chiral bis (ferrocenyl) ligands as voltammetric metal cation sensors<sup>[19]</sup>. The redox properties of ferrocenyl-substituted aryl azines were also investigated<sup>[20]</sup>. Frantz *et al.* studied the electrochemical behavior of phosphonic acids containing n-conjugated ferrocenyl unit grafted on metal oxides<sup>[21]</sup>. The redox properties of ferrocene-different saccharides and amino acid derivatives were investigated<sup>[22]</sup>. Electrochemistry of ferrocenylphosphines and some phosphine derivatives and metal complex derivatives were described<sup>[23]</sup>. Lipophilic macrocyclic host molecules containing multiple ferrocenyl redox-active centers were studied<sup>[24]</sup>.

The aim of the present work is an attempt to shed some additional light on the fundamental processes occurring on the electrode containing some reactive systems by the use of the AC impedance techniques, and verifying their applicability to elucidate heterogeneous parameters.

### Experimental:

Reagent-grade dichloromethane ( $\text{CH}_2\text{Cl}_2$ ), N,N-dimethylformamide (DMF) and acetonitrile (ACN) were further purified and dried according to a previous recommended method<sup>[26]</sup>. Tetrabutylammonium

perchlorate (TBAP) which was a Fluka product is recrystallised twice then vacuum dried at 120 °C.

For sample preparation and purification for electrochemical measurements in superdry media, a type of cell is frequently constructed and described elsewhere<sup>[26]</sup>. In this cell, three electrodes are used; the working electrode is either a platinum disc (Pt) or a metrohm EA 290 hanging mercury drop electrode [HMDE]. A platinum wire is used as an auxiliary electrode. The reference electrodes used were SCE and Ag/AgCl where its potential was calibrated for each experiment against the reversible oxidation peak of ferrocene.

An EG&G Princeton Applied Research 5208 Two-Phase Lock-in analyzer is used in conjunction with a computer controlled 273A Potentiostat/Galvanostat to perform the desired signals. A positive feedback which is installed inside the 273A is used in all the measurements to minimize the iR-drop effects.

The instrument was equipped with also an G&G 5208 Two Phase Lock-in Analyzer. The IS plots were recorded using an EPSON fx-850 Printer.

### RESULTS AND DISCUSSION

The values of both the charge transfer resistance and the warburg coefficient for pure solvent in the absence of electroactive substance and out of the faradaic region are extremely large. According to Randles model (Fig. 1) for an electrochemical cell, the Nyquist representation of IS crosses the  $Z'$  axis at  $R_\Omega$  with a phase angle of 90°.

Figure 2, shows the the Nyquist plots taken at the open circuit (against the reference electrode) and at frequencies ranging from 50 kHz and down to 10 Hz for 0.2 M TBAP in  $\text{CH}_2\text{Cl}_2$ ,  $\text{CH}_3\text{CN}$  and DMF. As can be observed from the curves, all the straight lines cross the  $Z'$  axis at a phase angle of nearly 90°. The results imply that the solvent resistance ( $R_\Omega$ ) is dependent of frequency. In addition, the double layer capacitance ( $C_{dl}$ ) is also frequency dependent but the values for the 3 solvents decrease with increasing the frequency. The IS data presents very small systematic departure from linearity at high frequencies ( $f > 5$  kHz), which can be ascribed to the geometry of the electrochemical cell, temperature as well as the size of both the auxillary and the working electrodes.

As can be observed from the table, the solvent resistance values under these conditions can not be correlated with their dielectric constant values. However, the solution resistance of the organic solvents can not be taken as an ideal resistance at least out of the faradaic potential region. However, it becomes insignificant near the standard potential  $E^\circ$  of the redox couple. The relation between the solvent resistance  $R_\Omega$

( $\Omega \text{ cm}^2$ ) and the reciprocal of the frequency of the AC potential ( $1/\omega$ ) for  $\text{CH}_3\text{CN}$  is also a straight line where its slope can be taken as a measure for the dependence of the solution resistance on frequency.

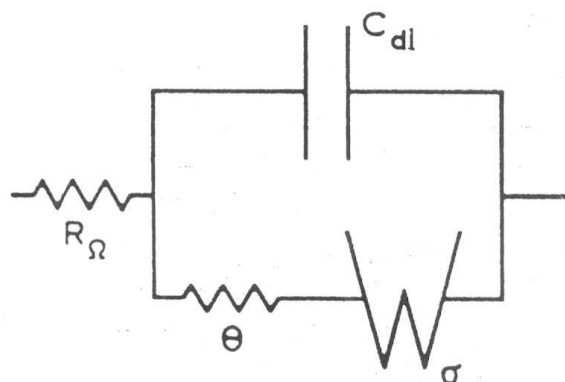


Fig. 1: The Randles equivalent circuit, which describes the responses of a single-step charge transfer process with diffusion of reactants and/or products to the interface

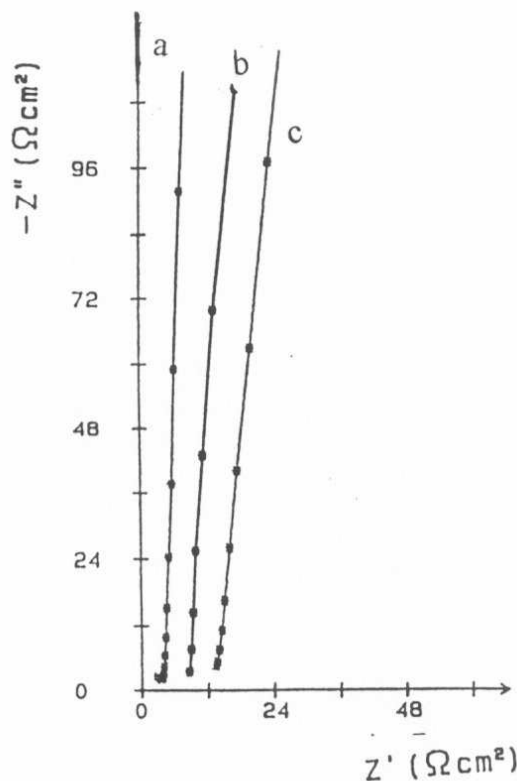


Fig. 2: IS diagram (Nyquist plot) for 0.2 M TBAP in pure aprotic solvents:

- a)  $\text{CH}_2\text{Cl}_2$
- b)  $\text{CH}_3\text{CN}$
- c) DMF

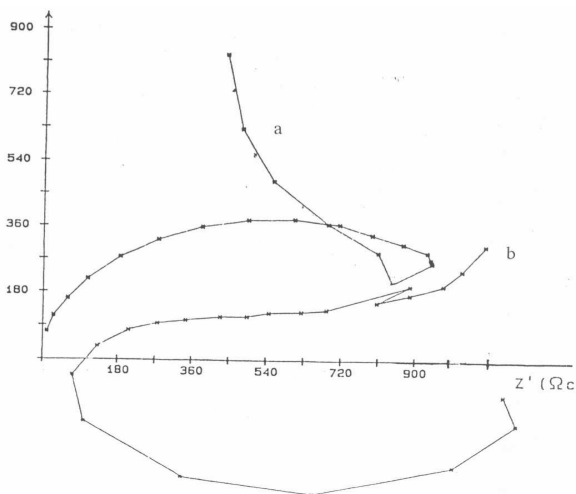


Fig. 3: IS diagram (Nyquist plot) obtained for the second oxidation step of 1mM of DPA in  $\text{CH}_2\text{Cl}_2/0.2 \text{ M TBAP}$ : a) at  $E_p$ . b) at 20 mV before  $E_p$

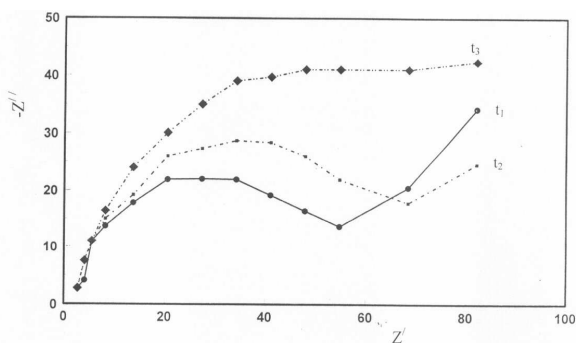


Fig. 4: Effect of time on the complex impedance plane plots of the reduction of 1mM of DPA in  $\text{CH}_3\text{CN}/0.2 \text{ TBAP}$  at Pt-disc electrode at 25 °C at the peak potential of the first step  
 $t_1 \sim 0.5 \text{ h}$        $t_2 \sim 5 \text{ h}$        $t_3 \sim 15 \text{ h}$

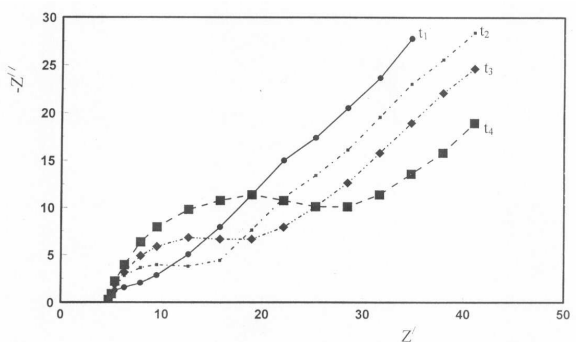


Fig. 5: Effect of time on the complex impedance plane plots of the oxidation of 0.5 mM of ferrocene in  $\text{CH}_3\text{CN}/0.2 \text{ TBAP}$  at Pt-disc electrode at 25 °C  
 $t_1 \sim 0.5 \text{ h}$     $t_2 \sim 5 \text{ h}$     $t_3 \sim 10 \text{ h}$     $t_4 \sim 15 \text{ h}$

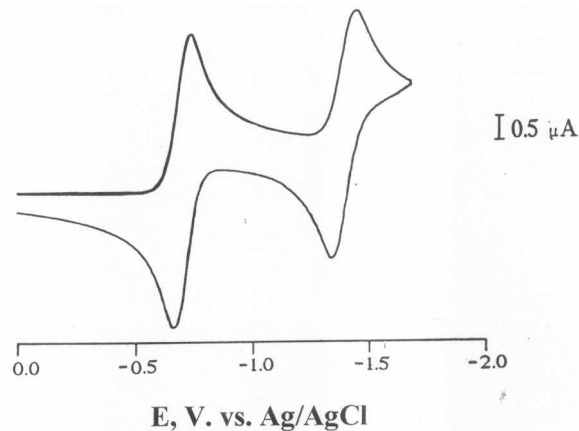


Fig. 6: Cyclic voltammogram of 0.5 mM of anthraquinone in  $\text{DMF}/0.2 \text{ TBAP}$  at Pt-disc electrode at 25 °C and scan rate = 200 mV/s

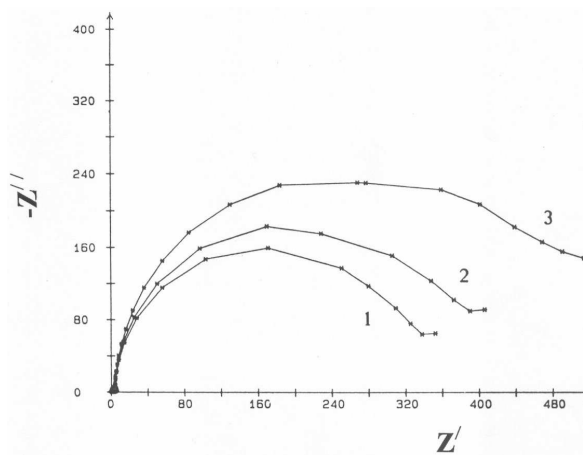


Fig. 7: Effect of time on the complex impedance plane plots of 0.5 mM of anthraquinone in  $\text{DMF}/0.2 \text{ TBAP}$  at Pt-disc electrode at 25 °C.  
 $t_1 \sim 0.5 \text{ h}$     $t_2 \sim 5 \text{ h}$     $t_3 \sim 10 \text{ h}$

Table 1: Double-layer capacitance values calculated for pure solvents

	$C_{dl}$ at 10 Hz/ $\mu\text{F}$	$C_{dl}$ at 50 kHz/ $\mu\text{F}$
$\text{CH}_2\text{Cl}_2$	8.6	7.3
$\text{CH}_3\text{CN}$	8.9	7.7
DMF	10.5	8.6

Table 2: solution-resistance values calculated for pure solvents

	$R_\Omega$ at 10 Hz/ $\Omega\text{cm}^2$	$R_\Omega$ at 5 kHz/ $\Omega\text{cm}^2$	DK
$\text{CH}_2\text{Cl}_2$	7.6	3.3	37.5
$\text{CH}_3\text{CN}$	10.8	8.5	9.1
DMF8.2	4.7	38	

The frequency-variation curve (Nyquist plot) of the oxidation of 2.2 mM of diphenylanthracene at the peak potential of its cyclic voltammogram (CV) in  $\text{CH}_2\text{Cl}_2/0.2 \text{ M TBAP}$  at 298 K, is given in Figure 3. The

values of IS at high frequencies fall in the fourth quadrant which means that the equivalent circuit characterizing this process must contain an inductive part in addition to that the charge transfer reaction must not be a simple process. On the other hand, the Nyquist plot at the peak-potential,  $E_p$ , of the first electron transfer, the results show linear behavior in the complex plane with an angle of  $45^\circ$  to the real axis.

Such a response is indicative of the presence of distributed elements in the material-electrode system, which corresponds to typically a reversible one-electron transfer reaction<sup>[17]</sup>. Under these conditions, the behavior can be related to the diffusion-controlled equation:  $Z = R_\Omega + \theta + \sigma\omega^{-1/2} + i(\sigma\omega^{-1/2} + 2\sigma^2 C_{dl})$ .

This confirms that the heterogeneous charge transfer rate constant,  $k_s$ , must be much greater than 0.01 cm/s as manifested by many studies.

The data depicted in Table 3 are evaluated from IS measurements for the oxidation of DPA at  $E_p$  to the radical cation in  $CH_2Cl_2$  using the following start values through a non-linear regression program.

$R_\Omega = 8.2$	$\Omega cm^2$	$C_{dl} = 9.0$	$\mu F$
$D = 8.8 * 10^{-6}$	$cm^2 s^{-1}$	$k_s = 2.0$	$cm/s$
$\alpha = 0.6$	$E^{1/2} = 1.3V. \text{ vs. Ag/AgCl.}$		

The ferrocene/ferrocenium redox couple has been often used in electron transfer studies as a reference systems in electrochemistry. This can be attributed to that the position of the peak potential of the redox pair is not greatly affected by changing parameters of the medium.

The previous works were concerned to measurements of the heterogeneous rate constants of electron transfer reactions<sup>[27-29]</sup>, where the  $k_s$ -values were ranged from 0.002 to 2.0 cm/s. But one has to keep in mind that the  $k_s$ - values measured using ultra micro-electrodes were clearly greater than those of the corresponding conventionally Pt-disc electrodes of the normal size. This can be attributed obviously to that passivation of the latter type through film formation on its surface is more observable than micro-electrodes. Measurements on ultra micro-electrode<sup>[30]</sup> in  $CH_3CN$

allowed the use of 0.1 to 50 mM of ferrocene where the calculated  $k_s$ -value was  $> 2$  cm/s. Its important to mention that the high concentration of ferrocene used has give rise to substantial passivation problems.

The Nyquist plot of the oxidation of ferrocene in  $CH_3CN/TBAP$  at the peak potential yields a straight line with an angle of nearly  $45^\circ$  with  $Z'$  axis. The IS data characterizes a diffusion-controlled process. The behavior reveal also that the heterogeneous rate constant must be greater than 0.01 cm/s.

The data depicted in Table 4 are evaluated from IS measurements for the oxidation of ferrocene at  $E_p$  in  $CH_2Cl_2$  using the following start values through a non-linear regression program.

$R_\Omega = 5.5$	$\Omega cm^2$	$C_{dl} = 5.8$	$\mu F$
$D = 1.2 * 10^{-5}$	$cm^2 s^{-1}$	$k_s = 1.5$	$cm/s$
$\alpha = 0.6$	$E^{1/2} = 0.63V. \text{ vs. Ag/AgCl.}$		

The data depicted in Table 5 are evaluated from IS measurement for the reduction of anthraquinone at  $E_p$  in DMF using the following start values through a non-linear regression program.

$R_\Omega = 6.5$	$\Omega cm^2$	$C_{dl} = 6.0$	$\mu F$
$D = 1.0 * 10^{-5}$	$cm^2 s^{-1}$	$k_s = 1.5$	$cm/s$
$\alpha = 0.5$	$E^{1/2} = -0.7V. \text{ vs. Ag/AgCl}$		

It is concluded that, the IS measurements in both acetonitrile and DMF are not reproducible as indicated by the results obtained in the complex plane at different intervals of time (Fig. 4, Fig. 5 and Fig. 7). The arcs become larger and the semicircles develop as the time of the experiment increases. On the basis of Randles model of an electrochemical cell, the charge transfer resistance of electron transfers process continuously increases and the kinetics of the charge transfer is becoming slower than ion diffusion in the electrolyte. The results show a single semicircle characteristic of kinetic control by an electrochemical charge transfer step at the electrode-electrolyte interface.

Table 3: Electrochemical parameters calculated for the first oxidation step of 2.2 mM (DPA) in  $CH_2Cl_2/0.2$  M TBAP at 298 K

$R_\Omega/\Omega cm^2$	$C_{dl}/\mu F$	$D/cm^2 s^{-1}$	$k_s/cm s^{-1}$	$\alpha$	$E^{1/2}/V.$
8.0	9.3	$9 * 10^{-6}$	2.2	0.55	1.31

Table 4: IS data collected for the oxidation of 1mM ferrocene in  $CH_2Cl_2/0.2$  M TBAP on Pt-disc electrode at 298 K

$R_\Omega/\Omega cm^2$	$C_{dl}/\mu F$	$D/cm^2 s^{-1}$	$k_s/cm s^{-1}$	$\alpha$	$E^{1/2}/V.$
5.7	5.5	$1 * 10^{-5}$	0.58	0.56	0.63

Table 5: IS data collected for the reduction of 0.8 mM anthraquinone to the radical anion in DMF/0.2 M TBAP on Pt-disc electrode at 298 K

$R_\Omega/\Omega cm^2$	$C_{dl}/\mu F$	$D/cm^2 s^{-1}$	$k_s/cm s^{-1}$	$\alpha$	$E^{1/2}/V.$
8.2	7.6	$1.4 * 10^{-5}$	1.3	0.52	-0.765

In this case, the development of the semicircles can be attributed to an increase of the passivation of the electrode surface through thin film formation<sup>[31]</sup>, partially due to the long time needed to perform valid measurements. It is found that, experiments carried out in methylene chloride are reproducible to about 15 hours, before some changes in IS results become significant.

This confirms the conclusion that other electrochemical techniques such as AC voltammetry or cyclic voltammetry have advantages over the electrochemical IS technique in evaluating kinetic parameters of charge transfer processes at least in some media.

### REFERENCES

1. Zeller, R.L. III and R.F. Sovinell, 1986. *Corros. Sci.*, 26: 591.
2. Epelboin, I., M. Keddam and H. Takinouti, 1972. *J. App. Electrochem.*, 2: 71.
3. Britton, C.F. and B.C. Tofield, 1988. *Mat. Performance*, 27: 41.
4. W. J. Lorenz and F. Mansfeld, *Corros. Sci.* 21 (1981) 647.
5. D. C. Silverman and J. E. Carrico, *Corrosion* 44 (1988) 280.
6. H. Gerischer, *Z. Physik. Chem.*, Leipzig, 198 (1951) 286.
7. G. H. Aylward, J. W. Hayes and R. Tamamushi; *Prac. of the 1<sup>st</sup> Austr. Conf.*, Pergamon Press, 1964, p. 323.
8. D. E. Smith, *Anal. Chem.*, 35 (1963) 602.
9. D. E. Smith in A. J. Bard (Ed), *Electroanalytical Chemistry*, vol. 1, Marcel Dekker, New York, 1966, chap. 1.
10. T. G. McCord and D. E. Smith, *Anal. Chem.*, 40 (1968) 1959.
11. B. Timmer, M. Sluyter-Rebach and J. H. Sluyters, *J. Electroanal. Chem.*, 18 (1968) 93.
12. B. Timmer, M. Sluyter-Rebach and J. H. Sluyters, *J. Electroanal. Chem.*, 19 (1968) 73.
13. R. De Levie and L. Pospisil., *J. Electroanal. Chem.*, 22 (1969) 277.
14. H. Moreira and R. De Levie, *J. Electroanal. Chem.*, 29 (1971) 353.
15. J. H. Sluyters and J. J. C. Oomen, *Rec. Trav. Chim.* 79 (1960) 1101.
16. A. J. Bard and L. R. Faulkner "Electrochemical Methods"; *Fundamentals and Applications*, Wiley & Sons, New York, 1980.
17. J. R. Macdonald "Impedance Spectroscopy"; *Emphasizing Solid Materials and Systems*, Wiley & Sons, New York 1987.
18. P. D. Beer, O. Kocian and R. J. Mortimer; *J. Chem. Soc. Dalton Trans.*, 11 (1990) 3283.
19. O. B. Sutcliffe, M. R. Bryce and A. S. Batsanov; *J. Organomet. Chem.*, 565:1-2 (2002) 211.
20. V. A. Sauro and M. S. Workentin; *Can. J. Chem.*, 80:3 (2002) 250.
21. R. Frantz, J. O. Durand, G. F. Lanneau, J. C. Jumas, O. F. Josette, M. Cretin and M. Persin; *Eur. J. Inorg. Chem.*, 5 (2002) 1088.
22. M. Chahma, J. S. Lee and H. B. Kraatz; *J. Organomet. Chem.*, 648: 1-2 (2002) 81-86.
23. A. J. Downard, N. J. Goodwin and W. Henderson; *J. Organomet. Chem.* 676: 1-2 (2003) 62-72.
24. P. D. Beer, A. C. Smythe, E. L. Tite and A. Ibbotson; *J. Organomet. Chem.*, 376 (1989) C11-C14.
25. J. F. Coetzee, *Recommended Methods for Purification of Solvents*, Pergamon, Oxford (1982).
26. F. Rashwan, *Doctoral Dissertation*, Freiburg University, West Germany, (1988).
27. K. M. Kadish, J. Q. Ding and T. Malinski; *Anal. Chem.* 56 (1984) 1741.
28. P. Cassoux, R. Cartiguepuyron, P.-L. Fabre and D. De Montauzon; *Electrochim. Acta*, 30 (1985) 2435.
29. A. M. Bond, T.L.E. Henderson and W. J. Thorman; *J. Phys. Chem.*, 90 (1986) 2911.
30. M. Sharp; *Electrochim. Acta*; 28 (1983) 301.
31. J. Daschbach, D. Blachwood and J. W. Pons; *J. Electroanal. Chem.*, 237 (1987) 269.